

# Chapter 5

## Porous Carbon Materials for Supercapacitor Applications



Manas Mandal, Krishna Chattopadhyay, Amrita Jain,  
and Swapan Kumar Bhattacharya

### 1 Introduction

With environmental consciousness, the advancement of energy conversion and storage has been a great challenge for the fulfillment of the enormous energy demand our modern society. Day-to-day discovery of portable electronics and smart technologies needs further breakthroughs to accomplish high power and energy and definitely long-running energy storage strategies. Recently, electrochemical capacitor, or supercapacitor, or ultracapacitors got tremendous attention toward materials science researchers as it has some unique features like high-power density, moderate energy density, fast charging capacity, and extraordinary cyclic stability [1–4]. Based on their charge storage phenomena, it can be categorized into two types: electrochemical double layer capacitors (EDLCs) and pseudocapacitors [5]. The charge accumulation at the interface of electrode/electrolyte results the capacitance in EDLCs, whereas the fast Faradaic redox reaction is responsible for the capacitance in pseudocapacitor. The transition metal oxides/hydroxides/sulfides and conducting polymers are used as

---

M. Mandal (✉)

Department of Chemistry, Sree Chaitanya College, North 24 Parganas, Habra,  
West Bengal 743268, India  
e-mail: [manasmandal26@gmail.com](mailto:manasmandal26@gmail.com)

M. Mandal · S. K. Bhattacharya (✉)

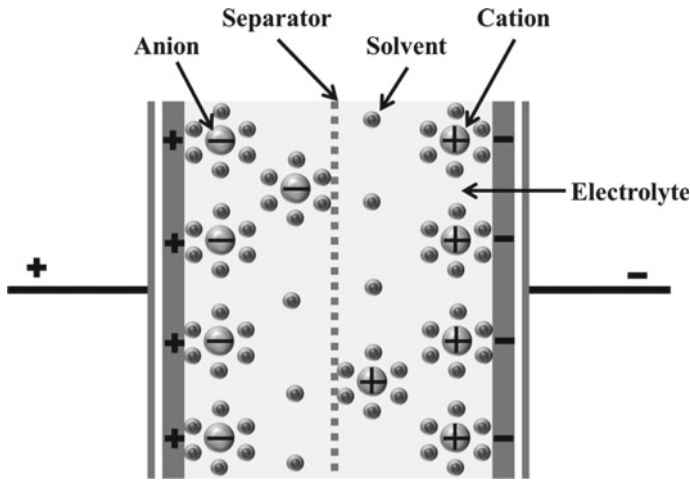
Physical Chemistry Section, Department of Chemistry, Jadavpur University, Kolkata, West  
Bengal 700032, India  
e-mail: [skbhatt7@yahoo.co.in](mailto:skbhatt7@yahoo.co.in)

K. Chattopadhyay

Department of Chemistry, University of Calcutta, 92 APC Road, Kolkata, West Bengal 700009,  
India

A. Jain

Institute of Fundamental Technological Research, Polish Academy of Sciences, Pawińskiego 5B,  
02-106 Warsaw, Poland



**Fig. 1** Schematic representation of carbon supercapacitors

pseudocapacitive materials. On the other hand, carbonaceous materials like activated carbon, graphene, carbon nanotube, aerogel etc., are used in EDLCs. Carbon supercapacitors assemble with two electrodes immersed in an aqueous or non-aqueous electrolyte and an electrolyte ion permeable porous membrane separator (Fig. 1).


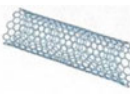
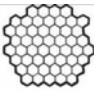
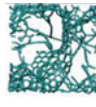
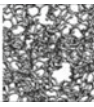
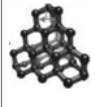
Carbon nanomaterials have been extensively developed in energy storage application because of its different architectures and tunable surface chemistry. Furthermore, it has high electrical conductivity, high electrochemical stability, excellent mechanical properties, and wide operating temperatures [6–8]. However, the most important criterion is the high specific surface area (SSA) of carbon materials for enhanced gravimetric capacitance. The different types of carbon-based materials with high SSA and high conductivity are depicted in Table 1 [9].

Every material has its unique structure and distinctive electrochemical properties. Such as zero- and one-dimensional carbon materials allow fast adsorption/desorption of the electrolyte ions on their surface, indicating high-power density. On contrary, two-dimensional graphene can deliver high charging/discharging rate and volumetric energy density. Porous 3D carbon materials acquire higher surface areas and mesoporous structure, providing higher energy densities [10].

## 2 Synthetic Strategies of Porous Carbon Materials

Porous carbon materials have been synthesized following different methods, viz., carbonization–activation methods, template methods, pyrolysis methods, etc.

**Table 1** Various types of carbon-based materials with their properties

Material	Carbon onions	Carbon nanotubes	Graphene	Activated carbon	Carbide derived carbon	Templated carbon
Dimensionality	0-D	1-D	2-D	3-D	3-D	3-D
Conductivity	High	High	High	Low	Moderate	Low
Volumetric capacitance	Low	Low	Moderate	High	High	Low
Cost	High	High	Moderate	Low	Moderate	High
Structure						

Reprinted with permission from Simon et al. [9]. Copyright 2013 American Chemical Society

## 2.1 Carbonization–Activation Methods

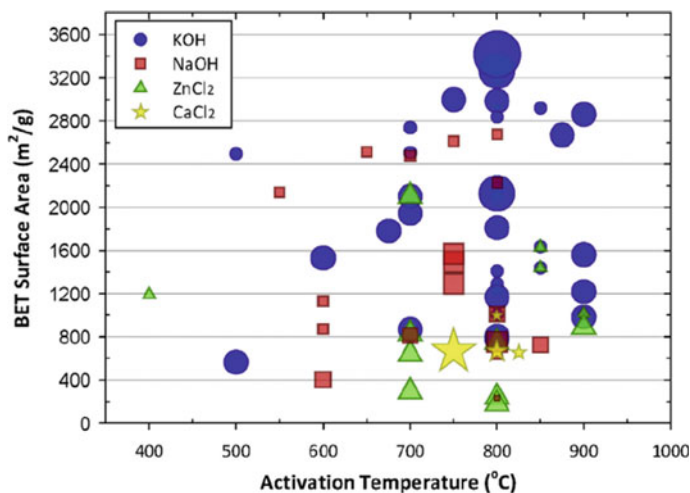
Generally, porous carbon prepared by this method is called activated carbon. The name of this process implies that it involves two different steps, viz., carbonization and activation. Carbonization produces the nonporous carbon material by pyrolysis, whereas the activation methods introduce the pores into the nonporous material chemically or physically forming activated carbon.

### 2.1.1 Carbonization

Carbonization is a method by which a carbonaceous residue is produced by thermal decomposition of organic substances (pyrolysis) under an inert atmosphere. A large number of different kinds of reactions like dehydrogenation, condensation, hydrogen transfer, crosslinking, and isomerization simultaneously occur during this process [11]. These various types of reactions help to release the volatile materials leaving behind the nonporous carbonaceous residue. This residue is also called as coal char or biochar.

### 2.1.2 Activation

In this step, the nonporous carbonaceous residue is treated with activating agents, also known as pore-forming agents or porogens. With activation agents, nonporous residue undergo oxidation reactions to create required pores into it. Based on the activating agents used in activation methods, these are categorized as either chemical or physical activation method [13]. The chemical activation process uses KOH, NaOH, Na<sub>2</sub>CO<sub>3</sub>, K<sub>2</sub>CO<sub>3</sub>, ZnCl<sub>2</sub>, or H<sub>3</sub>PO<sub>4</sub> as activating agents, whereas CO<sub>2</sub>, O<sub>2</sub>,



**Fig. 2** BET surface area vs activation temperatures of porous carbons for different chemical porogens (KOH, NaOH, ZnCl<sub>2</sub>, and CaCl<sub>2</sub>). Reprinted with permission from Gao et al. [12]. Copyright 2018 Elsevier

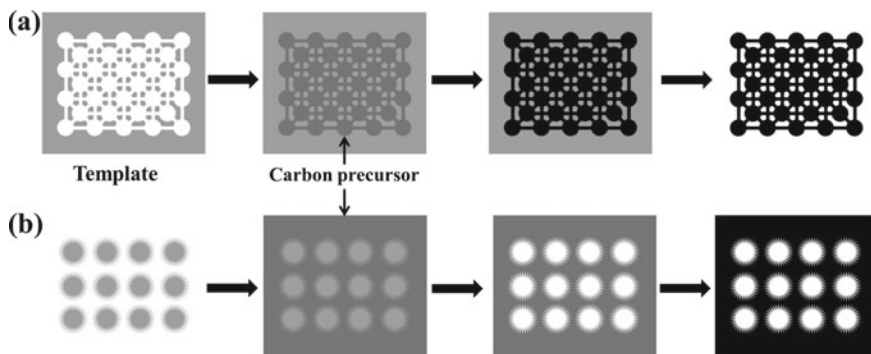
air, or steam in physical activation. Both the processes have several advantages and disadvantages as well. The chemical activation is comparatively low-temperature process which produces highly meso-porous carbon with high mass of yields and Brunauer–Emmett–Teller (BET) surface area (Fig. 2). On contrary, physical activation requires high activation temperatures with longer time and produces relatively lower yields with small pore sizes and low specific surface area (SSA). In spite of these advantages, physical activation process is more feasible and useful for industrial scale production than chemical activation, as it exhibits low corrosion.

## 2.2 Template Methods

Template methods are well-known approach by which morphological information is transferred from a pre-prepared template to the derived porous carbon.

### 2.2.1 Hard Templates

The hard template method, also known as nanocasting, is an efficient route for the preparation of porous carbons with highly uniform pore structure and pore size distributions. However, this method is costly and laborious as it includes various steps. The important steps involved in this method are (i) synthesis of a hard template with specific morphology, (ii) good contact of the template with carbon sources, (iii)



**Fig. 3** Schematic diagrams of ordered meso-porous carbon preparation using **a** hard template and **b** soft template methods

heating at high temperature under inert conditions, and (iv) acid or alkali etching of the template (Fig. 3a). The extreme stability of the hard templates toward a very high-temperature facilitates the preparation of highly crystalline or sometimes single-crystal materials using this process. Templates with uniformly ordered porous structure can be easily prepared using  $\text{SiO}_2$  [14, 15],  $\text{ZnO}$  [16, 17],  $\text{MgO}$  [18, 19],  $\text{TiO}_2$  [20],  $\text{Al}_2\text{O}_3$  [21, 22] or zeolite [23], etc.

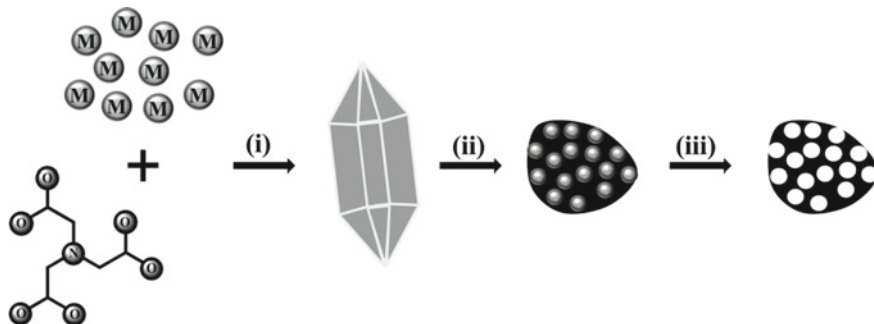
### 2.2.2 Soft Templates

Soft templates do not have solid shapes like hard template. Generally, block copolymers (BCPs) or self-assembly of amphiphilic small molecules are used to prepare soft templates under appropriate condition. In addition of proper solvent, these molecules turn into micelles due to strong interaction forces, such as hydrophilic and hydrophobic interactions [24], hydrogen bonding [25], and electrostatic interactions [26] between them. Then, the micelles blended with carbon precursor result in heterogeneous matrix which produces porous carbon materials during the carbonization (Fig. 3b). The size and architecture of the pores can be tuned by varying the ratio of solvent and micelle. Therefore, a soft template should have the capability to accumulate into nanostructures and supporting the porogens of soft template before the development of carbon skeleton. Dai and coworkers successfully synthesized the ordered meso-porous carbons (OMCs) by soft template technique using micelles of amphiphilic block copolymers for the first time [27].

### 2.2.3 Self-template Methods

In activation methods and hard/soft template methods, a pore generator chemical species, known as porogen, is required. The self-template method uses in situ

self-generated porogens to synthesize the porous carbon without addition of any external porogens. The metal–organic frameworks (MOFs), ethylenediaminetetraacetates (EDTA)-based salts, biomass-based organic salts, etc., are used as self-generated porogens in self-template methods. These materials serve as both a source and a spontaneous template for the final carbon material. Therefore, self-template synthesis of porous carbon includes following steps: (i) precipitation, (ii) pyrolysis, and (iii) washing (Fig. 4). The organic ligands are carbonized to produce the carbon matrix. During washing, the inorganic atoms or particles are washed out to form meso- and macro-pores. J ayaramulu et al. reported two-dimensional nanoporous carbon sheets (NPSs) from rod-shaped potassium-based MOF  $\{K_3[C_6H_3(CO_2)(CO_2H_{0.5})(CO_2H)]_2\}(H_2O)_2$  (denoted as K-MOF). The 2D NPSs were obtained upon two-step carbonization process at 450 °C and 800 °C where K-containing rod-shaped hollow structure and 2D NPSs were formed, respectively. Potassium was removed by etching with 5 wt% HCl followed by washing the product with a water–ethanol mixture for several times [28]. The as-prepared porous sample having a BET surface area of 1192 m<sup>2</sup> g<sup>-1</sup> showed excellent electrochemical performances. The highest specific capacitance for the sample was calculated to be 233 F g<sup>-1</sup> at scan rate of 5 mVs<sup>-1</sup> in 1 M H<sub>2</sub>SO<sub>4</sub> electrolyte with good rate capability. Yu et al. used ethylenediaminetetraacetic acid disodium zinc salt (EDTANa<sub>2</sub>Zn) for the preparation of hierarchical porous carbons (N-doped) by direct pyrolysis. The EDTANa<sub>2</sub>Zn acts as C-precursor, N-source, as well as porogen [29]. Pyrolysis generated nano-ZnO and Na<sub>2</sub>CO<sub>3</sub> act as self-template to form meso-pore in carbon matrix. The sample prepared at 700 °C, having BET surface area of 1368 m<sup>2</sup> g<sup>-1</sup> with high N-content showed a maximum specific capacitance of 275 F g<sup>-1</sup> with excellent rate capability in 6 M KOH electrolyte.



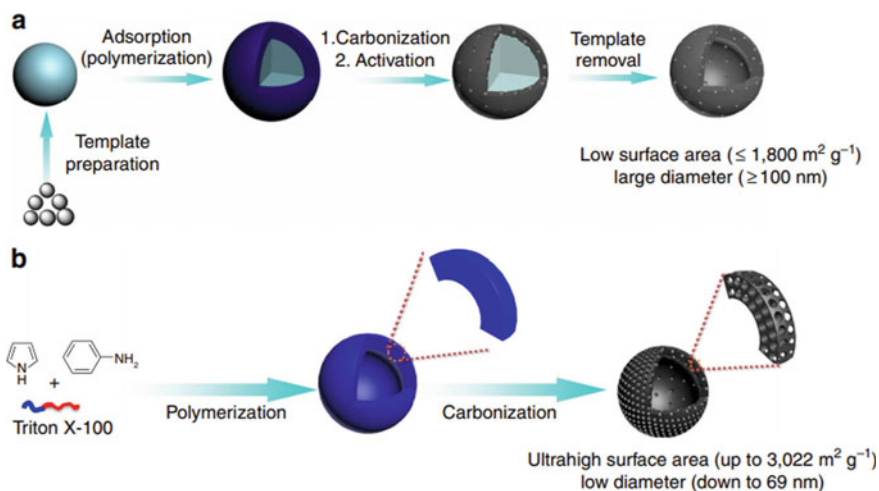
**Fig. 4** Schematic diagrams for the self-template synthesis of porous carbon including precipitation (i) pyrolysis, (ii) washing, and (iii) steps

## 2.3 Pyrolysis Methods

Although, the porous carbon with uniform pore size distribution and high specific surface area can be prepared using traditional carbonization–activation methods and templating methods, the porogens or the template need to be removed completely (Fig. 5). In that context, pyrolysis methods are more useful. During pyrolysis method, organic sources are decomposed and release gases like  $\text{CO}_2$ ,  $\text{H}_2\text{O}$ ,  $\text{NH}_2$ , and  $\text{CO}$ . These produced gases act as porogens. By optimizing the pyrolysis parameters, like heat rate, temperature, and time of carbonization, the pore size distribution and specific surface area of the porous carbon can be fine-tuned. Xu et al. prepared distinct hollow carbon nanospheres with surface area of  $3022 \text{ m}^2 \text{ g}^{-1}$  following a simple carbonization of polyaniline-co-polypyrrole (PACP) hollow spheres [30]. The as-prepared materials achieved the maximum specific capacitance of  $203 \text{ F g}^{-1}$  at specific current of  $0.1 \text{ A g}^{-1}$ .

## 3 Typical Features of Carbon Materials for Supercapacitors Electrode

The porous carbon materials are an emerging electrode of supercapacitor because of its exceptional chemical and physical properties, such as high SSA with controlled



**Fig. 5** Schematic illustration for the preparation of conventional hollow carbon nanosphere by **a** templating method and **b** by pyrolysis method. Reprinted with permission from Xu et al. [30]. Copyright 2015 Springer Nature

pore structure, high electrical conductivity, good corrosion resistance, easy processability and compatibility in composite, high-temperature stability, and relatively low cost [31].

### 3.1 Large Surface Area

Different types of porous carbon materials have been developed as promising active materials for supercapacitor application. Ordered meso-porous carbons (OMCs) with a precise range of pore sizes have comparatively large SSA ( $\sim 1000 \text{ m}^2 \text{ g}^{-1}$ ) that provides the double layer capacitance. Carbon aerogels having surface area ranging from 500 to 800  $\text{m}^2 \text{ g}^{-1}$ , with comparatively small pore sizes is unfavorable for electrolyte ion diffusion. On contrary, macro-porous carbon materials have relatively lower surface area ( $\sim 600 \text{ m}^2 \text{ g}^{-1}$ ). Among all types of porous carbons, mixed porous carbon like activated carbon with micro-, meso-, and macro-pores show the largest SSA ( $\sim 3000 \text{ m}^2 \text{ g}^{-1}$ ) and high electrochemical activity in terms of specific capacitance, energy, and power thereof [32].

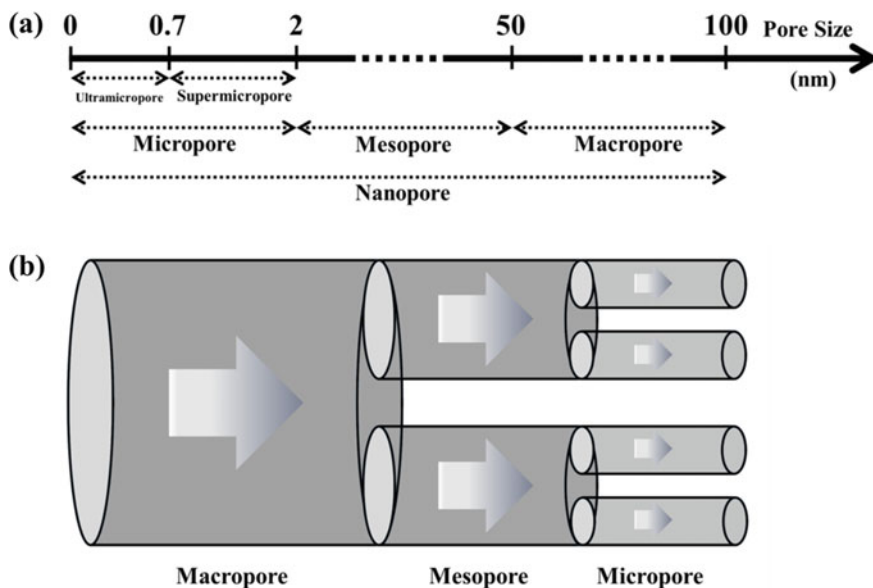
### 3.2 Hierarchical Porosity

Hierarchical porosity implies the presence of multi-scale pores having different sizes in a porous system. The pores with the diameter of smaller than 100 nm are known as nanopores. Based on the width or diameter ( $d_{\text{pore}}$ ) of pores, the International Union of Pure and Applied Chemistry (IUPAC) classified these nanopores into following (Fig. 6a) [33]:

- (i) Micro-pore: The pore having diameters less than 2 nm ( $d_{\text{pore}} < 2 \text{ nm}$ ). This type of pores is again classified into two types: ultra micro-pore ( $d_{\text{pore}} < 0.7 \text{ nm}$ ) and super micro-pore ( $0.7 \text{ nm} < d_{\text{pore}} < 2 \text{ nm}$ ).
- (ii) Meso-pore: The pore having diameters greater than 2 nm and lesser than 50 nm ( $2 \text{ nm} < d_{\text{pore}} < 50 \text{ nm}$ ).
- (iii) Macro-pore: The pore having diameters greater than 50 nm and lesser than 100 nm ( $50 \text{ nm} < d_{\text{pore}} < 100 \text{ nm}$ ).

In hierarchical porous carbons (HPCs), not only the presence of multi-scale pores but also an interconnection between them is an essential criteria to form a hierarchical network. These interconnected pores are beneficial for the infiltration of the electrolytes [34]. So that it can provide high electrochemically accessible surface area and decrease the ion diffusion path. An ion diffusion path in the hierarchical porous material is schematically represented in Fig. 6b, where the electrolyte ions enter the macro-pore first and then goes into the smaller pores which are directly interconnected. In an electrochemical capacitor, the macro-, meso- and micro-pores



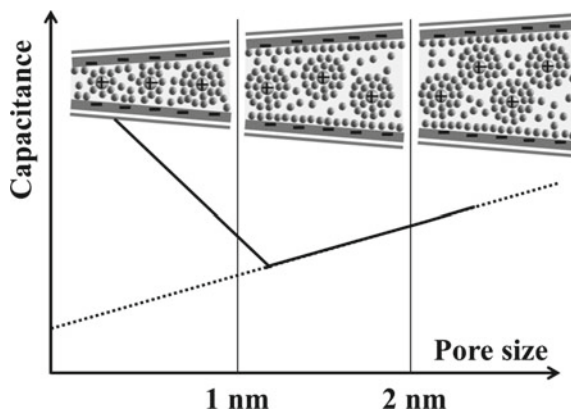


**Fig. 6** **a** Different kinds of nanopores based on IUPAC scale. **b** Schematic diagram of an ion diffusion path in a hierarchical porous material

play important roles individually and contribute to the total capacitance (Fig. 7). The micro-pores provide large surface area which acts as the main sites for the charge accumulation, whereas macro-pores and meso-pores serve as the ion-buffering reservoirs and provide channels for the rapid ion transport, respectively [34–36]. The macro-pores acting as the ion-buffering reservoirs store the electrolyte ions for meso-/micro-pores, and therefore, an easy and rapid ion transfer occur by reducing the effective diffusion pathways and enhance the electrochemical performance. Generally, the fast ion transport provides high specific power and the rate capability of the supercapacitor electrode. The time for the ion transport ( $\tau$ ) greatly depends on its diffusion coefficient ( $D$ ) and transport path ( $L$ ) according to the equation:  $\tau = L^2/D$ . Therefore, the superior ion transport kinetics can be achieved by reducing the ion transport path and enhancing the ion diffusion coefficient [37].

However, the pore size has the important role in determining the capacitance for porous carbon supercapacitor. If the size of the pore is bigger ( $\sim$ doubled) than the diameters of the hydrated electrolyte ions, also termed as solvated ions or solvation shell, is beneficial for higher capacitance. Because the high pore size allows the formation of double layer within the pore. The value of the capacitance decreases with decreasing the pore size. But when the size of the pore is much smaller ( $\sim$ 1 nm) than the solvated ions, capacitance is sharply increased. This is due to the distortion of the solvated ions in the smaller pore resulting in closer approach of the ion center to the active surface area of the electrode [38]. The research by Raymundo-Piñero et al. supports the above fact, and they showed that an ample size of pore is more significant

**Fig. 7** General trend of the capacitance value with pore size of the porous carbon



to achieve high capacitance in different types of electrolyte. They reported that the effective optimal pore size is  $\sim 0.7$  nm and  $\sim 0.8$  nm in case of aqueous (KOH) and organic (tetraethylammonium tetrafluoroborate, TEABF<sub>4</sub> in acetonitrile) electrolyte, respectively [39].

### 3.3 Electrochemical Performance in Different Electrolytes

Porous carbon electrode has excellent electrochemical stability in different types of electrolytes with wide range of operating potential. The main factor on which the operating potential window depends is electrolyte. As the decomposition potential of water is 1.23 V, the supercapacitor devices can be operated up to 1.2 V in traditional aqueous electrolyte like KOH, H<sub>2</sub>SO<sub>4</sub>. However, the neutral aqueous electrolyte such as Na<sub>2</sub>SO<sub>4</sub> provides the maximum operating voltage up to 1.9 V [40]. The common organic electrolytes such as TEABF<sub>4</sub> in acetonitrile or polycarbonate are suitable for the operating voltage as high as 3 V [41]. The different types of electrolytes affect the electrochemical performances of the porous carbon supercapacitor differently. Chen et al. investigated the electrochemical performances of biomass-derived porous carbon in different aqueous-based such as KOH, H<sub>2</sub>SO<sub>4</sub>, Na<sub>2</sub>SO<sub>4</sub>, and organic electrolyte, tetraethylammonium tetrafluoroborate in propylene carbonate (Et<sub>4</sub>NBF<sub>4</sub>/PC) [42]. Due to smaller size of solvated H<sup>+</sup> and K<sup>+</sup> ions, the porous carbon showed high capacitance in H<sub>2</sub>SO<sub>4</sub> and KOH electrolyte. Although the bigger size of Et<sub>4</sub>N<sup>+</sup> and BF<sub>4</sub><sup>-</sup> is not suitable for high capacitance, but it shows high rate capability due to shorter ion diffusion path. The higher operating potential of Et<sub>4</sub>NBF<sub>4</sub>/PC and Na<sub>2</sub>SO<sub>4</sub> helps to achieve high energy density according to the formula  $E = 1/2CV^2$ . Another class of electrolyte, i.e., ionic liquids has drawn great interest as a promising electrolyte because of their some unique properties such as high thermal stability, non-flammability, low vapor pressure, intrinsic ionic conductivity, and excellent operational voltage greater than 3 V [43]. The electrochemical

**Table 2** Electrochemical performances of the porous carbon supercapacitor in various electrolytes

Electrode	Electrolyte	Potential	Capacitance	References
Hierarchical PC	6 M KOH	1.0 V	338.5 F g <sup>-1</sup> at 1 A g <sup>-1</sup>	[44]
N, O, P-doped PC	1 M Na <sub>2</sub> SO <sub>4</sub>	1.9 V	69.8 F g <sup>-1</sup> at 0.1 A g <sup>-1</sup>	[40]
PC network	1 M Et <sub>4</sub> NBF <sub>4</sub> in acetonitrile	2.7 V	208 F g <sup>-1</sup> at 0.75 A g <sup>-1</sup>	[45]
Hierarchical PC	1 M H <sub>2</sub> SO <sub>4</sub>	1.0 V	266 F g <sup>-1</sup>	[42]
	1 M Na <sub>2</sub> SO <sub>4</sub>	1.6 V	211 F g <sup>-1</sup>	
	6 M KOH	1.0 V	309 F g <sup>-1</sup>	
	1 M Et <sub>4</sub> NBF <sub>4</sub> /PC	2.5 V	168 F g <sup>-1</sup> at 0.5 A g <sup>-1</sup>	
Meso-porous graphene	EMIMTFSI	4.0 V	244 F g <sup>-1</sup> at 5 A g <sup>-1</sup>	[46]
Micro-pore-rich activated carbon	EMIMFSI	3.5 V	120 F g <sup>-1</sup> at 0.5 A g <sup>-1</sup>	[47]
Hierarchical PC	EMIMBF <sub>4</sub>	3.8 V	217 F g <sup>-1</sup> at 0.1 A g <sup>-1</sup>	[48]

TEABF<sub>4</sub>/PC: Tetraethylammonium tetrafluoroborate in propylene carbonate; EMIMTFSI: 1-ethyl-3-methylimidazolium bis(trifluoromethylsulfonyl)imide; EMI-FSI: 1-ethyl-3-methylimidazolium bis(fluorosulfonyl)imide; EMIMBF<sub>4</sub>: 1-ethyl-3-methylimidazolium tetrafluoroborate; PC: Porous carbon

performances of different porous carbon supercapacitor in various electrolytes are depicted in Table 2.

### 3.4 Different Kinds of Morphology

High-surface area is really essential for supercapacitor electrodes, but to get maximum capacitance, whole surface area should be accessible to the electrolyte ions. But practically, it is not achievable. To increase the surface accessibility, the surface topography can be modified with abundant adsorbing sites. Therefore, significant research efforts have been devoted to engineering diverse carbon morphologies with controlled surface topography and interior texture.

#### 3.4.1 One-Dimensional Porous Carbon Electrode

Due to the unique anisotropic properties, one-dimensional (1D) porous carbon materials such as carbon nanofibers, carbon nanorods carbon nanowires, and carbon nanobelts have many advantages over the other nanostructures. These 1D nanostructures can deliver fast axial electron transport and provide short ion diffusion path, high ion-accessible specific surface area and excellent mechanical strength. The contact resistance is greatly reduced due to the more exposed edges which

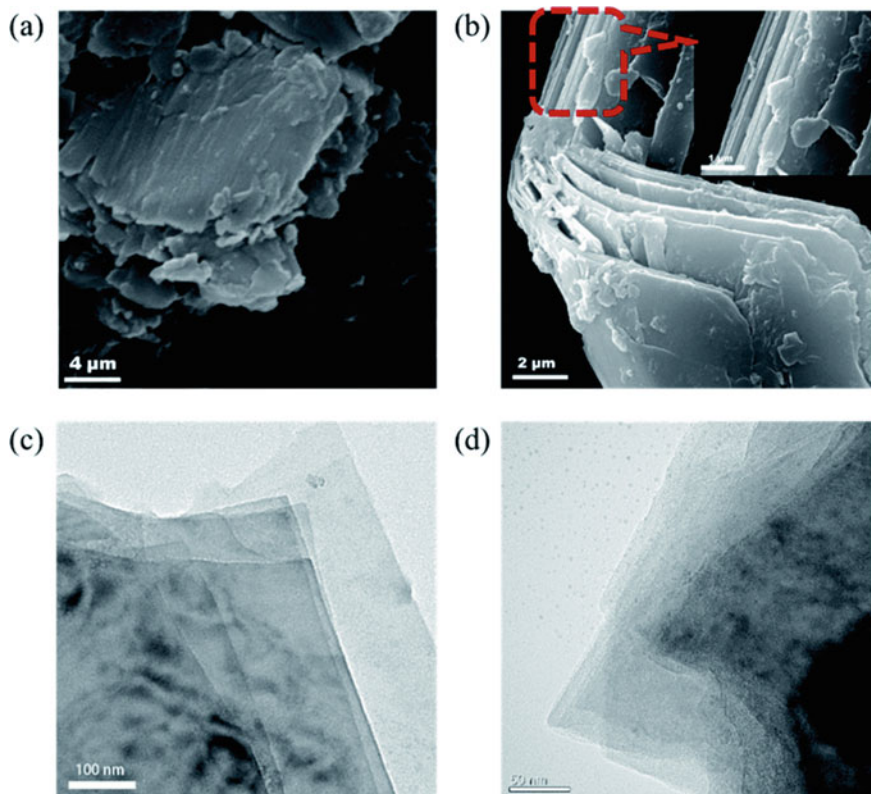
behave as contact points. Furthermore, surface functionalization can be easily done chemically to improve the electrochemical performance.

Na et al. fabricated nitrogen and fluorine doped carbon nanofibers by a simple hydrothermal treatment followed by carbonization and vacuum plasma process [49]. The as-prepared material exhibited meso-porous nature with highest BET specific surface area of  $596.1 \text{ m}^2 \text{ g}^{-1}$ . It also exhibited maximum specific capacitance of  $252.6 \text{ F g}^{-1}$  at  $0.5 \text{ A g}^{-1}$  in  $1 \text{ M H}_2\text{SO}_4$  electrolyte. Cai et al. reported inter-bonded carbon nanofibers for high-performance supercapacitor. They first prepared cellulose nanofibers by electrospinning method using cellulose acetate solution. In second step, the desired porous materials were synthesized by hydrothermal treatment followed by carbonization process. The as-prepared material exhibited maximum specific capacitance of  $241.4 \text{ F g}^{-1}$  at specific current of  $1 \text{ A g}^{-1}$  with excellent cyclic stability [50]. Using lignin as precursor, Berenguer et al. fabricated flexible interconnected porous carbon fibers with high SSA and excellent conductivity. The desired electrode material was prepared by electrospinning method followed by thermostabilization and carbonization treatments. The interconnected nature of the fibers helps to increase the charge transfer process and electrochemical performances as well [51]. Micro- and meso-porous 1D carbon nanobelts with high SSA up to  $1208 \text{ m}^2 \text{ g}^{-1}$  were synthesized by “stripping and cutting” strategy from tofu using a molten salt-assisted technique by Ouyang and coworkers. This material achieved high specific capacitance of  $262 \text{ F g}^{-1}$  at specific current of  $0.5 \text{ A g}^{-1}$  with high cyclic stability [52]. Jin et al. fabricated wood-based fibers by melt-spinning process and then finally prepared the activated carbon fibers by carbonization-activation at  $850 \text{ }^\circ\text{C}$  under steam–nitrogen mixture [53]. Comparatively, longer activation time produces highly meso-porous structure, which is easily reachable by the electrolyte ions up to the inner micropores. The as-prepared materials exhibited maximum capacitance of  $280 \text{ F g}^{-1}$  at  $0.5 \text{ A g}^{-1}$  with excellent stability.

### 3.4.2 Two-Dimensional Porous Carbon Electrode

Two-dimensional (2D) porous carbon materials are excellent in energy storage which can provide high conductivity due to their  $sp^2$  hybridized nature, high SSA with high electrochemically active sites.

Fan et al. reported 2D porous carbon nanosheets supercapacitor with superior rate performance. They prepared the porous material following a combined method of intercalation, thermal treatment, and potassium hydroxide activation using montmorillonite as nano-template and gelatin as carbon source. The porous nature of the nanosheets reduces the ion transport path and enhances the pore accessibility toward electrolyte ions and thus achieved excellent rate performance, with a high specific capacitance of  $246 \text{ F g}^{-1}$  at a ultrahigh specific current of  $100 \text{ A g}^{-1}$  [54]. Xu and coworkers synthesized layered 2D porous carbon materials (Fig. 8) by a wet-chemical synthesis method using Sonogashira–Hagihara cross-coupling polycondensation. The BET surface specific area of the as-prepared material was measured



**Fig. 8** SEM (a, b) and TEM images (c, d) of 2D porous carbon material at different magnifications. Reprinted with permission from Xu et al. [55]. Copyright 2021 Royal Society of Chemistry

to be  $575 \text{ m}^2 \text{ g}^{-1}$  with hierarchical pore structure. The electrode material achieved high specific capacitance of  $378 \text{ F g}^{-1}$  at the specific current of  $0.1 \text{ A g}^{-1}$  [55].

### 3.4.3 Three-Dimensional Porous Carbon Electrode

Three-dimensional ordered porous carbon (3D-OPC) has shown remarkable potential in energy storage and conversion applications due to its some unique properties like large SSA with uniform pore structure, high electronic and ionic conductivity, and low cost.

Zhao et al. reported three-dimensional hierarchical ordered porous carbons (3D HOPCs) using templating technique. They used nano-array of silica ( $\text{SiO}_2$ ) sphere, triblock copolymer P123 and sucrose as hard template, soft template, and carbon source, respectively. The 3D HOPCs having SSA of  $1182 \text{ m}^2 \text{ g}^{-1}$  achieved maximum specific capacitance of  $247 \text{ F g}^{-1}$  at specific current of  $1 \text{ A g}^{-1}$  with excellent rate

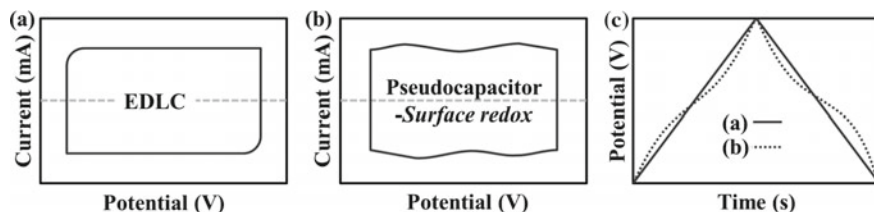
performance. Moreover, the 3D HOPCs supercapacitors showed high percentage (91%) of capacitance retentions after consecutive 10,000 cycles [56]. Li et al. prepared three-dimensional graphene-like carbon nanosheet network using a surfactant (Tween-20) as C source. The as-prepared material acquired hierarchical porous structure with a SSA of 2017.3 m<sup>2</sup> g<sup>-1</sup> [57]. It exhibited ideal capacitive behavior with maximum specific capacitance of 316.8 F g<sup>-1</sup> at a specific current of 1 A g<sup>-1</sup> in 1 M KOH electrolyte.

### 3.5 Electrochemical Characteristics of Porous Carbon Supercapacitors

Generally, supercapacitor stores charge in two ways: (i) via Faradaic fast electron transfer or/and (ii) via non-Faradaic charge storage mechanism. However, each type of supercapacitor can be identified from their electrochemical characteristics in terms of cyclic voltammograms (CVs) and galvanostatic charge/discharge (GCD) curves [58]. In general, a pure porous carbon electrode shows electrical double layer capacitive behavior giving rectangular CV curve (Fig. 9a) and a triangular-shaped GCD curve indicating linear voltage response (Fig. 9c). Usually, EDLCs exhibit the capacitance which is potential-independent and so is the obtained current in CV plot. However, surface functional groups/doping atoms on the carbon can add pseudocapacitance and therefore deviations from its ideal electrochemical signatures in terms of CV curve (Fig. 9b) and GCD curve (Fig. 9c) occur.

#### 3.5.1 Capacitance of Porous Carbon Supercapacitor

There are many ways by which capacitance of a supercapacitor can be expressed like specific or gravimetric capacitance, volumetric capacitance, and areal capacitance. The gravimetric capacitance which depends upon the mass of the active material is usually expressed in Farads per gram (F g<sup>-1</sup>), whereas the areal capacitance depends upon the foot print area, and the capacitance values are expressed in Farads per square centimeter (F cm<sup>-2</sup>). Furthermore, the volumetric capacitance is calculated



**Fig. 9** Schematic CV curve of **a** EDLC, **b** pseudocapacitor, and **c** corresponding galvanostatic charge–discharge curves

per volume, and the values are indicated in  $\text{F cm}^{-3}$ . Depending upon the application and necessity, the values are expressed differently, but gravimetric and areal capacitances are the two mostly used units to express capacitance of a device. The calculation of the capacitance also depends upon the type of working electrode used. There are certain scenarios where the calculation of areal capacitance can be difficult, for example, when metal foams are used as substrate and also for porous materials. On the other hand, gravimetric capacitance requires the exact mass of the electrode material used during the capacitance calculation. Though both the techniques are not free from errors, each technique has their own set of advantages and disadvantages when it comes to design and structure of the working electrode.

The electrochemical performance in terms of gravimetric capacitance of the porous carbon materials can be improved by increasing the SSA or the ample pore size. However, the volumetric capacitance is limited due to low bulk density of porous carbon [59]. But it is important to have the high volumetric capacitance for the practical applications. Therefore, doping with heavier heteroatoms is a highly effective method for the enhancement of the density of the porous carbon which leads to enhanced volumetric capacitance (Table 3).

## 4 Understanding of Charge Storage Mechanisms in Porous Carbon

### 4.1 *Electrochemical Double Layer Model Using 2D Electrode Materials*

The first electrochemical double layer model (EDL) was given by Helmholtz [72], and in his model, he explained the phenomenon of the charge separation which takes place at the interface of electrode–electrolyte, assuming that the surface of the electrode is planar. Helmholtz model is picturized in Fig. 10a, and from the figure, it can be seen that the charges those are accumulated at the surface of the electrode are counterbalanced by the electrostatic absorption with the ions of electrolyte which results in the formation of oppositely charged two-layers at the interface. Concept of this study was very similar to the traditional parallel plate capacitors, and therefore, the capacitance of Helmholtz layer is given by using Eq. 1:

$$\frac{C}{A} = \frac{\epsilon_r \epsilon_0}{d} \quad (1)$$

where,  $\epsilon_0$  ( $8.85 \times 10^{-12} \text{ F m}^{-1}$ ) is the vacuum permittivity,  $\epsilon_r$  is the dielectric constant of the electrolyte material which is dimensionless,  $d$  (m) is the average distance between the conductive layers, and  $A$  ( $\text{m}^2$ ) is the surface area of the electrode which is accessible.

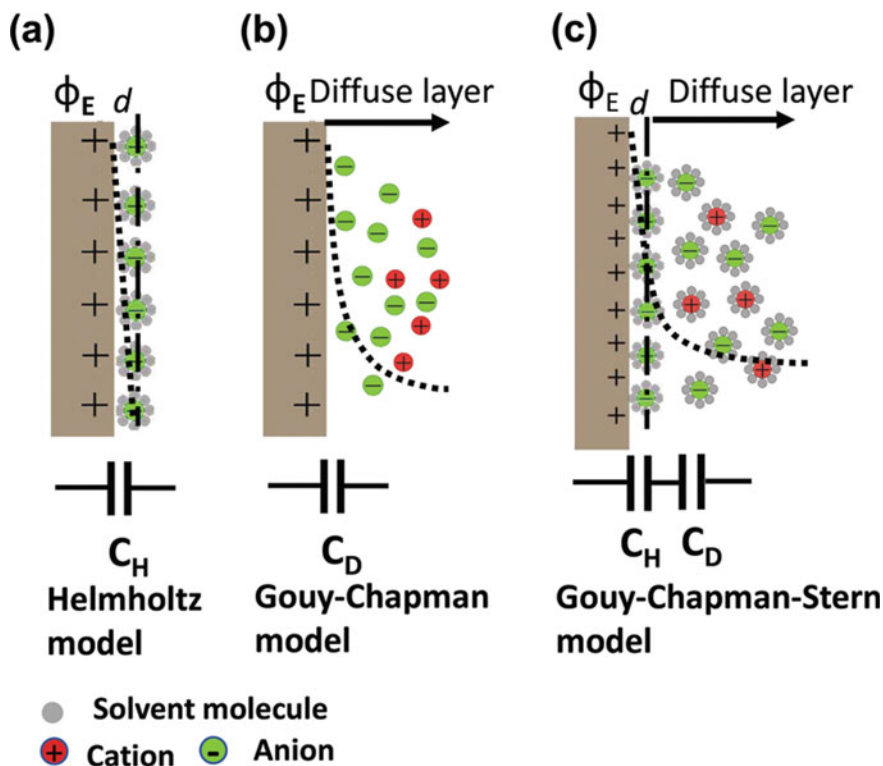
**Table 3** Comparison between the gravimetric and volumetric capacitances of reported porous carbon materials

Electrode	Electrolyte	Gravimetric capacitance	Volumetric capacitance	Specific current/scan rate	Reference
N-doped PC nanosheets	6 M KOH	305 F g <sup>-1</sup>	287 F cm <sup>-3</sup>	2 mV s <sup>-1</sup>	[60]
P, N-doped PC	1 M H <sub>2</sub> SO <sub>4</sub>	205.7 F g <sup>-1</sup>	261 F cm <sup>-3</sup>	0.5 A g <sup>-1</sup>	[61]
PC	6 M KOH 1.5 M Et <sub>4</sub> NBF <sub>4</sub> /AN	271 F g <sup>-1</sup> 156 F g <sup>-1</sup>	252 F cm <sup>-3</sup> 145 F cm <sup>-3</sup>	2 mV s <sup>-1</sup>	[62]
Micro-porous carbon	1 M H <sub>2</sub> SO <sub>4</sub>	198 F g <sup>-1</sup>	180 F cm <sup>-3</sup>	2 mV s <sup>-1</sup>	[63]
PC	6 M KOH	262 F g <sup>-1</sup>	214 F cm <sup>-3</sup>	0.05 A g <sup>-1</sup>	[64]
High density porous graphene macroform	6 M KOH	238 F g <sup>-1</sup>	376 F cm <sup>-3</sup>	0.1 A g <sup>-1</sup>	[65]
N, P, S-doped hierarchically PC Spheres	6 M KOH	274 F g <sup>-1</sup>	219 F cm <sup>-3</sup>	0.5 A g <sup>-1</sup>	[66]
N, P, O-doped PC spheres	6 M KOH 0.5 M H <sub>2</sub> SO <sub>4</sub>	356.9 F g <sup>-1</sup> 434.7 F g <sup>-1</sup>	760 F cm <sup>-3</sup> 925 F cm <sup>-3</sup>	1 A g <sup>-1</sup> 0.1 A g <sup>-1</sup>	[67]
N, S-doped hierarchical PC	6 M KOH	358.0 F g <sup>-1</sup>	243.4 F cm <sup>-3</sup>	0.5 A g <sup>-1</sup>	[68]
N-doped hierarchical PC	1 M H <sub>2</sub> SO <sub>4</sub>	242 F g <sup>-1</sup>	306 F cm <sup>-3</sup>	0.5 A g <sup>-1</sup>	[69]
Hierarchical pomegranate-like PC	4 M H <sub>2</sub> SO <sub>4</sub>	398 F g <sup>-1</sup>	278.6 F cm <sup>-3</sup>	0.5 A g <sup>-1</sup>	[70]
F, N-doped PC nanosheets	1 M H <sub>2</sub> SO <sub>4</sub>	266 F g <sup>-1</sup>	255 F cm <sup>-3</sup>	1 A g <sup>-1</sup>	[71]

Et<sub>4</sub>NBF<sub>4</sub>/AN: Tetraethylammonium tetrafluoroborate in acetonitrile; PC: Porous carbon

Depending on the electrolyte used, the value of the dielectric constant  $\epsilon_r$  and thickness ( $d$ ) of the Helmholtz layer is used to normalize the areal capacitance (per m<sup>2</sup>) of the Helmholtz layer ( $C_H$ ). For example, the dielectric constant value of water is around 78 [73], and for most of the solvents used for EDC application, this values lies in between 1 and 100 at room temperature [73–75]. Usually, this value is not so important at sub-nanometer scale; even sometimes, it is smaller than that of bulk electrolyte [73]. In the Helmholtz model, linear potential drop taking place between Helmholtz layer is also discussed, however, the charges which are in excess at the surface of the electrode are usually not completely compensated by the Helmholtz layer, especially when the concentration of solution is not so high [74]. Moreover, it is difficult to have a single stable compact layer from counter ion layer from electrolyte as ions in the electrolyte are always in movement because of thermal





**Fig. 10** Schematic diagram of electrochemical double layer model: **a** Helmholtz model, **b** Gouy-Chapman model, and **c** Gouy-Chapman-Stern model. Reprinted with permission from Shao et al. [7]. Copyright 2020 Royal Society of Chemistry

fluctuation. Further improvement in this model was done by Gouy-Chapman [76, 77]; in their model, they have introduced a new layer called as diffused layer between the electrode and the bulk electrolyte, taking into consideration of the thermal fluctuation as per the Poisson-Boltzmann equation [1]. The Gouy-Chapman model was presented in Fig. 10b. The distribution of ions on the diffuse layer highly depends on the distance because of the electrostatic attractions which decreases from the surface of the electrode to the bulk of the electrolyte. In case of monovalent electrolytes, the average thickness of the so-called diffuse layer also called as Debye length;  $\lambda_D$  is given as

$$\lambda_D = \sqrt{\frac{\varepsilon_r \varepsilon_0 RT}{2(ZF)^2 C_0}} \quad (2)$$

where  $\varepsilon_0$  is the vacuum dielectric constant ( $F m^{-1}$ ) and  $\varepsilon_r$  is the relative permittivity of the electrolyte.  $R$  ( $J mol^{-1}$ ) is the ideal gas constant,  $T$  (K) is the absolute

temperature,  $F$  ( $\text{C mol}^{-1}$ ) is the Faraday constant, and  $C_0$  ( $\text{mol m}^{-3}$ ) is the bulk electrolyte concentration. Diffuse layer capacitance  $C_D$  can be calculated from the Poisson-Boltzmann equation which can be written as

$$C_D = \frac{\varepsilon_r \varepsilon_0}{\lambda_D} \cosh\left(\frac{zF\phi}{2RT}\right) \quad (3)$$

where  $\phi$  (V) is the electrical potential,  $F$  ( $\text{C mol}^{-1}$ ) is the Faraday's constant,  $R$  ( $\text{J mol}^{-1}$ ) is the ideal gas constant,  $T$  (K) is the temperature, and  $\varepsilon_0$  and  $\varepsilon_r$  are the vacuum and relative dielectric constant ( $\text{F m}^{-1}$ ). As per Eq. (3), differential capacitance  $C_D$  is not considered as a constant, instead, this model suggested a "U" shape of the differential capacitance with respect to the potential of the electrode, which is in-line with the experimental results, obtained using NAF solutions with Hg in low concentration [78]. Also the capacitance which was experimentally measured with liquid electrolytes was far below from the prediction from the model [79]. The main shortcoming of this model was to consider that point charges can virtually reach to the surface at zero distance which in turn leads to the infinite value of capacitance. To fix these issues, Stern improvised the model of Gouy-Chapman by taking into consideration the real size of ions as a result of which an additional compact layer called as Stern layer was created which is in series with diffuse layer, this arrangement can be seen from Fig. 10c [80]. This compact layer (Stern layer) is very much similar to Helmholtz layer from the point of physics, having thickness of  $x_H$  (m). The electrochemical double layer capacitance from this model is given by the following equation:

$$\frac{1}{C_{DL}} = \frac{1}{C_H} + \frac{1}{C_D} = \frac{X_H}{\varepsilon_0 \varepsilon_r} + \frac{\lambda_D}{\varepsilon_0 \varepsilon_r \cosh\left(\frac{zF\phi}{2RT}\right)} \quad (4)$$

where  $C_H$  is the capacitance of Stern (Helmholtz) layer and  $C_D$  is the capacitance of diffuse layer, these capacitance are measured in  $\text{F m}^{-2}$ . Overall electrochemical double layer capacitance is calculated by calculating the smallest capacitance obtained between  $C_H$  and  $C_D$ . In case of highly concentrated electrolytes, thickness of the diffuse layer drops to zero, so the Helmholtz capacitance is the only one to be considered. For sure, Gouy-Chapman-Stern model was a milestone that predicted a more realistic gross feature of the EDL, and the theoretical observations were close to experimental results. But this model also suffers from some limitations, like this model has not considered the ion-ion correlation effects, which are very important especially in solvent-free ionic liquid-based electrolyte systems [74, 81]. Similarly, considering a linear potential drop within the compact layer was inappropriate in high electrode polarization with high concentration electrolytes [74, 82]. Whatsoever, the Gouy-Chapman-Stern model has provided a constructive and well predicted interpretation of the electrochemical double layer that has certainly helped us in developing EDLC field from last few decades.

## 4.2 Capacitance in Nanoporous Carbon-Derived Electrodes

There are many factors which decide the overall electrochemical performance of nanoporous carbon-derived EDLC electrodes, like electrical conductivity, presence of the surface groups, and the most important are the BET specific surface area (SSA), pore size, and pore size distribution. Though most of the carbon materials possess high conductivity because they have high density of electronic state at Fermi level, but still there exist some carbon materials which have semiconducting properties like SWCNTs which has specific diameter and also specific helicity or bilayer graphene [83, 84]. Because of this semiconducting nature, the drop of the current near potential of zero charge is usually seen in a cyclic voltammogram curve (CV), and because of this, a CV which is closed to butterfly shape is obtained in a three-electrode system, and a trapezoid-shaped CV is seen in a two-electrode system [73]. In general, the capacitance value of carbon-based electrode in electrochemical double layer capacitor cell is strongly dependent on the surface area of material and pore size and structures of the material, and therefore, a detailed characterization of the surface and textual properties is utmost important to analyze how the specific surface area, pore size, and its structures affect the electrochemical performance of carbon-based supercapacitor cells. Although the porous carbon is usually complex materials with different kind of structures which includes local graphitized and disorder arrangements of carbon, and hence, it is impracticable and tough to predict their local structures (in real) and long-range structures [85, 86]. However, there are now various kind of experimental techniques which are well developed and sufficiently advanced to predict and analyze the materials up to great extent like gas sorption, electron microscopy, NMR, neutron scattering, X-ray scattering, and in situ techniques [87]. In addition to the experimental techniques, modeling and simulation methods like density functional theory, pair distribution function, Monte Carlo method, and gas sorption techniques are the most widely used to study the pore structures of porous carbon materials in more detail ways [87].

## 4.3 Capacitance with Respect to Specific Surface Area (SSA)

Gouy, Chapman and Stern proposed in their model that the overall double layer capacitance achieved is directly proportional to the specific surface area of the material used, and this theory triggered the race to enhance the specific surface area of the active material which will in turn increase the overall capacitance values. Several research groups had developed their interest in activated carbon and the activation techniques by which the surface area and pore volume can be increased. But, after some time, it was realized that the gravimetric capacitance of active material was limited even if the most porous samples which has very high surface area were used [88–91]. Ji et al. studied that the area-normalized capacitance was decreased by 4–5  $\mu\text{F cm}^{-2}$  when the SSA was above 1500  $\text{m}^2 \text{g}^{-1}$  [92]. This is usually because

of the presence of micro-pores, specially narrow sub-nanometer size micro-pore in porous carbon was too small to accommodate the ions of electrolyte [93, 94]. As a conclusion, still, there are no clear trends established between specific area and capacitance.

#### ***4.4 Capacitance with Respect to Pore Size***

There is a quite established proposition which states that it is always preferred to have pore size of active material (for example, carbon in case of EDLCs) larger than the solvated ion size of electrolyte, as in this scenario, pores of active materials are accessible to electrolyte ions [90]. In other words, carbon materials whose pore sizes are smaller than the solvated electrolyte ions do not contribute to capacitance, and hence, they are considered as useless. If we take into account, the most commonly used electrolytes; the size of free ions and ions with solvated shells varies in between few to tens of Å. For example, the size of free tetraethylammonium cation is around 0.68 nm, and when it is dissolved in acetonitrile, the size increased to 1.3 nm. Clearly in this situation, large micro-pore and meso-pore carbons are considered as an ideal candidate for achieving high capacitance value.

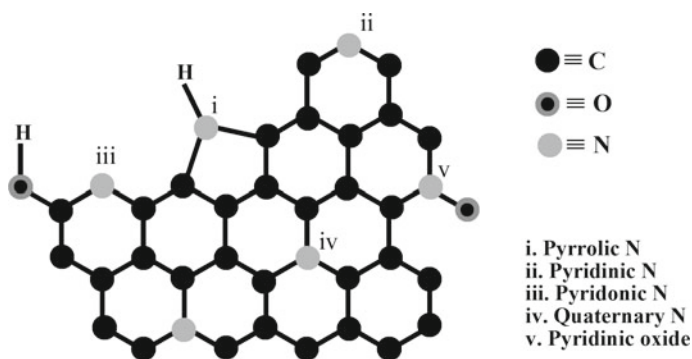
### **5 Structure–activity Relationship with Heteroatom Doped Carbon Materials**

Although the prediction on acquiring capacitance is much higher, the volumetric and gravimetric capacitance of carbon nanomaterials are restricted to  $400 \text{ F cm}^{-3}$  [95] and  $300 \text{ F g}^{-1}$  [96], respectively. This is because of sole involvement of physical charge storage phenomena without any contribution of fast Faradaic redox reactions. Therefore, doping with heteroatoms could be an effective strategy for the enhancement of capacitance. The charge storage mechanism in porous carbon is discussed in Sect. 4. However, self-doped porous carbon from various biomass precursors or doping with heteroatoms like, O, N, P, B during activation process adds some more advantages like enhanced wettability due to polarized surface, improved intrinsic conductivity, and better electrochemical performances resulting from the introduction of faradaic pseudocapacitance of the redox active sites [97]. The structural distortions and electronic structure modulations generally occur due to the size and electronegativity differences between the dopant atoms and carbon. The total electrochemically active surface of the electrode material where electrolyte ions are accumulated is defined as “electrolyte infiltration” [98]. The porous hierarchical polar surface resulting from heteroatom doping facilitates a fast and adequate electrolyte infiltration which establishes multidirectional pathways for rapid ion transfer and therefore improves the

electrochemical performance. The electrolyte infiltration is directly related to the wettability of an electrolyte which is measured by contact angle meter [99].

The enhancement of electrochemical performances of oxygen doped carbon materials is mainly due to the increasing wettability of the electrode material to the electrolyte, fast Faradaic redox reactions contributing pseudocapacitance, and increased pore utilization ratio. However, oxygen functionalization can decrease the surface conductivity and prevent the electrolyte ions from entering the pore. He et al. thoroughly investigated the reasons for capacitance enhancement in oxygen containing carbon nanofibers. In acidic aqueous electrolyte,  $H_3O^+$  ion attracts the electrons on the O atom of the functional groups, and therefore charge separation occurs which facilitates the redox reaction. While the adsorption/desorption reaction of the hydrated ions of alkaline aqueous electrolyte in the pore causes the pseudocapacitance [100]. Wang et al. investigated the pseudocapacitive behavior of the O-doped carbon cloth which was prepared by annealing the carbon cloth in presence of air at low temperatures. They concluded that micro-pores having oxygen functional groups can give high pseudocapacitance than surface of pristine carbon plane, by facilitating the faradaic redox reactions due to increased ion-accessible area [101].

Nitrogen-doping in porous carbon materials distorts the structure and creates defects and available active sites. Doping with nitrogen atom can cause a shift of the Fermi level toward valence band in carbon materials, accelerating the electron transfer [102]. It can also enhance the wettability by increasing the polarity and charge density of the materials. In carbonaceous material, generally, five types of N-functionalization are encountered, such as pyrrolic nitrogen (N-5), pyridinic nitrogen (N-6), pyridonic nitrogen (N-5), quaternary or graphitic nitrogen (N-Q), and pyridinic oxide (N-X) (Fig. 11) [103]. Due to the electron donating nature, pyridinic and pyrrolic nitrogens serve as electroactive center in electrochemical capacitor. The graphitic nitrogen helps to improve the electronic conductivity and creates additional defects. However, all types of nitrogen can add pseudocapacitance to the total capacitance [104].



**Fig. 11** Schematic illustration of N atom doped porous carbons

Liu et al. prepared N-doped porous carbons from pyrrole and Na-metal using a three-step process which involves solvothermal, pyrolysis, and acid washing of metal salts. The meso-porous carbons with high specific surface areas of  $2000 \text{ m}^2 \text{ g}^{-1}$  were obtained at high-temperature pyrolysis. The as-prepared materials perform as excellent electrode materials for supercapacitor with exceptional rate performances, long lifetime, and high-power density [105]. Zhu et al. prepared high-level N-doped (up to 8.71%) micro-porous carbon materials having high specific surface areas by a facile Schiff-base reaction of 3,3'-diaminobenzidine and p-phthalaldehyde in ethanol solvent and a subsequent single-step carbonization-activation process. The as-prepared material exhibited high gravimetric capacitance with excellent rate capability and electrochemical stability [106].

The electrochemical activities of different heteroatoms doped porous carbon materials are depicted in Table 4. Although there is no linear relation between the heteroatom types/content and supercapacitive performances, the electrochemical activity is greatly enhanced by doping with heteroatoms like O, N, S, and B.

## 6 Conclusions and Prospects

Supercapacitors are getting enormous importance as these can make a bridge between a conventional capacitor and a battery. Porous carbon materials offer low-cost electrode materials having high SSA ( $1500\text{--}2000 \text{ m}^2 \text{ g}^{-1}$ ) and extraordinary electrochemical performances. For the porous carbon-based supercapacitive electrodes, the conventional synthesis strategies like carbonization-activation, templating methods, salient features to act as electrode in supercapacitors, and heteroatom functionalization have been discussed in this chapter.

Generally, physical activation methods are used to produce porous carbon electrodes for commercial purpose. The porogens like  $\text{H}_2$ ,  $\text{CO}_2$ , and air are used in physical activation to create porous carbons with high SSA. The porogens used in chemical activation methods do the same job as physical porogens do but they are highly toxic in nature and produce various pollutants during chemical activation. Therefore, the chemical activation method requires environment friendly green methods to prepare porous carbons at a reasonable cost.

Recently, the porous carbon doped with heteroatom such as O, N, S, and B have been thoroughly investigated for the supercapacitor materials. The introduction of these heteroatoms improves the electrochemical performances of the material by increasing electronic mobility, extrinsic defects, and wettability. However, the functional mechanisms of porous carbon electrodes doped with different heteroatom are largely dependent on their size and electronegativity difference. Therefore, an appropriate choice of dopants with their relative ratios is highly desirable.

The capacitance of porous carbon supercapacitor mainly comes from the fast and reversible ion adsorption-desorption at the carbon/electrolyte interfaces. For the enhancement of the electrochemical performances, the interface accessibility and

**Table 4** Supercapacitive performances of porous carbon materials doped with heteroatoms

Electrode material	Heteroatom content	Surface area ( $\text{m}^2\text{g}^{-1}$ )	Specific capacitance ( $\text{F/g}$ ) at specific current ( $\text{A g}^{-1}$ ) or scan rate ( $\text{mVs}^{-1}$ )	Electrolyte	Reference
N-rich meso-porous Carbons	N: 19.10 wt%	458	252 at $0.2 \text{ A g}^{-1}$	1 M $\text{H}_2\text{SO}_4$	[107]
N and B co-doped PC	N: 15–20%, B: 10–13%	955	188 at $0.5 \text{ A g}^{-1}$	6 M KOH	[108]
N-doped PC nanofibrous microspheres	N: 2.4 at.%, O: 6.1 at.%	1147	113 at $5 \text{ mVs}^{-1}$	EMIMTFSI	[109]
Honeycomb-like PC foam	N: 1.1 at.%, O: 11.2 at.%	1313	260 at $2 \text{ mVs}^{-1}$	1 M $\text{Na}_2\text{SO}_4$	[110]
N/S-doped PC	N: 4.5 at.%, S: 5.8 at.%	1339	464 at $0.2 \text{ A g}^{-1}$	6 M KOH	[111]
N-doped PC superstructures	N: 3.46 wt%, O: 7.99 wt%	1375	364 at $0.6 \text{ A g}^{-1}$	6 M KOH	[112]
N-doped micro-porous carbon spheres	N: 8.71 at.%, O: 7.89 at.%	1478	292 at $1 \text{ A g}^{-1}$	6 M KOH	[106]
PC nanorods	N: 1.47 at.%, O: 0.62 at.%	1559	187 at $0.05 \text{ A g}^{-1}$	1 M $\text{H}_2\text{SO}_4$	[113]
N/S-co-doped carbon nanobowls	N: 3.3 wt%, S: 1.7 wt%	1567	279 at $0.1 \text{ A g}^{-1}$	6 M KOH	[114]
3D interconnected S-doped PC	S: 5.2 wt%	1592	320 at $0.2 \text{ A g}^{-1}$	6 M KOH	[115]
N-doped PC nanosheets	N: 2.10 at.%, O: 7.11 at.%	1786.1	339 at $0.25 \text{ A g}^{-1}$	6 M KOH	[116]
N-doped multi-chamber carbon microspheres	N: 4.58 wt%, O: 2.12 wt%	1797	301 at $0.2 \text{ A g}^{-1}$	6 M KOH	[117]
2D PC nanosheets	N: 1.54 at.%, O: 6.59 at.%	1907	221 at $1 \text{ A g}^{-1}$	EMIMBF <sub>4</sub>	[118]
N and S-co-doped hierarchical PC	N: 1.88 at.%, S: 1.87 at.%	1975	333.4 at $0.1 \text{ A g}^{-1}$	6 M KOH	[119]
S-doped PC nanosheets	S: 9.6 wt%	2005	312 at $0.5 \text{ A g}^{-1}$	6 M KOH	[120]
B/N-co-doped carbon nanosheets	N: 3.1 at.%, B: 0.5 at.%	2362	235.6 at $0.5 \text{ A g}^{-1}$	1 M $\text{Na}_2\text{SO}_4$	[121]

(continued)

**Table 4** (continued)

Electrode material	Heteroatom content	Surface area ( $\text{m}^2\text{g}^{-1}$ )	Specific capacitance (F/g) at specific current ( $\text{Ag}^{-1}$ ) or scan rate ( $\text{mVs}^{-1}$ )	Electrolyte	Reference
N-rich PC nanosheets	N: 9.4 at.%, O: 4.7 at.%	2406	250 at $0.5\text{ A g}^{-1}$	EMIMBF <sub>4</sub>	[122]

EMIMTFSI: 1-ethyl-3-methylimidazolium bis(trifluoromethylsulfonyl)imide; EMIMBF<sub>4</sub>: 1-ethyl-3-methylimidazolium tetrafluoroborate; PC: Porous carbon

carbon/electrolyte compatibility should be highly improved. Therefore, the introduction of nanopores to the porous carbon material and doping pseudo-active sites improves the interfacial interactions.

**Acknowledgements** MM thanks to Sree Chaitanya College, Habra for giving permission to carry out the research work. KC acknowledges Ishaan Mandal for allowing enough time for literature survey and writing the draft during this pandemic.

## References

1. Conway BE (2013) Electrochemical supercapacitors: scientific fundamentals and technological applications. Springer Science & Business Media
2. Majumdar D, Mandal M, Bhattacharya SK (2019)  $\text{V}_2\text{O}_5$  and its carbon-based nanocomposites for supercapacitor applications. *Chem Electro Chem* 6(6):1623–1648
3. Mandal M, Ghosh D, Chattopadhyay K, Das CK (2016) A novel asymmetric supercapacitor designed with  $\text{Mn}_3\text{O}_4$ @ multi-wall carbon nanotube nanocomposite and reduced graphene oxide electrodes. *J Electron Mater* 45(7):3491–3500
4. Mandal M, Maitra A, Das T, Das CK (2015) Graphene and related two-dimensional materials. In: Graphene materials: fundamentals and emerging applications. John Wiley & Sons, Inc, pp 3–23
5. Mandal M, Ghosh D, Giri S, Shakir I, Das CK (2014) Polyaniline-wrapped 1D  $\text{CoMoO}_4 \cdot 0.75\text{H}_2\text{O}$  nanorods as electrode materials for supercapacitor energy storage applications. *RSC Adv* 4(58):30832–30839
6. Miao L, Song Z, Zhu D, Li L, Gan L, Liu M (2020) Recent advances in carbon-based supercapacitors. *Mater Adv* 1(5):945–966
7. Shao H, Wu YC, Lin Z, Taberna PL, Simon P (2020) Nanoporous carbon for electrochemical capacitive energy storage. *Chem Soc Rev* 49(10):3005–3039
8. Feng HP, Tang L, Zeng GM, Tang J, Deng YC, Yan M, Liu YN, Zhou YY, Ren XY, Chen S (2018) Carbon-based core-shell nanostructured materials for electrochemical energy storage. *J Mater Chem A* 6(17):7310–7337
9. Simon P, Gogotsi Y (2013) Capacitive energy storage in nanostructured carbon–electrolyte systems. *Acc Chem Res* 46(5):1094–1103
10. Gogotsi Y (2015) Not just graphene: the wonderful world of carbon and related nanomaterials. *MRS Bull* 40(12):1110–1121



11. Alslaibi TM, Abustan I, Ahmad MA, Foul AA (2013) A review: production of activated carbon from agricultural byproducts via conventional and microwave heating. *J Chem Technol Biotechnol* 88(7):1183–1190
12. Gao M, Pan SY, Chen WC, Chiang PC (2018) A cross-disciplinary overview of naturally derived materials for electrochemical energy storage. *Mater Today Energy* 7:58–79
13. Yin J, Zhang W, Alhebshi NA, Salah N, Alshareef HN (2020) Synthesis strategies of porous carbon for supercapacitor applications. *Small Methods* 4(3):1900853
14. Schmidt-Winkel P, Lukens WW, Zhao D, Yang P, Chmelka BF, Stucky GD (1999) Mesocellular siliceous foams with uniformly sized cells and windows. *J Am Chem Soc* 121(1):254–255
15. Liang HW, Wei W, Wu ZS, Feng X, Mullen K (2013) Mesoporous metal–nitrogen-doped carbon electrocatalysts for highly efficient oxygen reduction reaction. *J Am Chem Soc* 135(43):16002–16005
16. He S, Zhang C, Du C, Cheng C, Chen W (2019) High rate-performance supercapacitor based on nitrogen-doped hollow hexagonal carbon nanoprism arrays with ultrathin wall thickness in situ fabricated on carbon cloth. *J Power Sources* 434:226701
17. Yu S, Wang H, Hu C, Zhu Q, Qiao N, Xu B (2016) Facile synthesis of nitrogen-doped, hierarchical porous carbons with a high surface area: the activation effect of a nano-ZnO template. *J Mater Chem A* 4(42):16341–16348
18. He X, Li R, Qiu J, Xie K, Ling P, Yu M, Zhang X, Zheng M (2012) Synthesis of mesoporous carbons for supercapacitors from coal tar pitch by coupling microwave-assisted KOH activation with a MgO template. *Carbon* 50(13):4911–4921
19. Geng W, Ma F, Wu G, Song S, Wan J, Ma D (2016) MgO-templated hierarchical porous carbon sheets derived from coal tar pitch for supercapacitors. *ElectrochimActa* 191:854–863
20. de Almeida FC, Zarbin AJ (2006) Hollow porous carbon microspheres obtained by the pyrolysis of TiO<sub>2</sub>/poly (turfuryl alcohol) composite precursors. *Carbon* 44(14):2869–2876
21. Fang Y, Lv Y, Che R, Wu H, Zhang X, Gu D, Zheng G, Zhao D (2013) Two-dimensional mesoporous carbon nanosheets and their derived graphene nanosheets: synthesis and efficient lithium ion storage. *J Am Chem Soc* 135(4):1524–1530
22. Liang Y, Schwab MG, Zhi L, Mugnaioli E, Kolb U, Feng X, Müllen K (2010) Direct access to metal or metal oxide nanocrystals integrated with one-dimensional nanoporosity for electrochemical energy storage. *J Am Chem Soc* 132(42):15030–15037
23. Ania CO, Khomeiko V, Raymundo-Piñero E, Parra JB, Beguin F (2007) The large electrochemical capacitance of microporous doped carbon obtained by using a zeolite template. *Adv Funct Mater* 17(11):1828–1836
24. Zhao Y, Jiang L (2009) Hollow micro/nanomaterials with multilevel interior structures. *Adv Mater* 21(36):3621–3638
25. Chu WC, Bastakoti BP, Kaneti YV, Li JG, Alamri HR, Allothman ZA, Yamauchi Y, Kuo SW (2017) Tailored design of bicontinuous gyroid mesoporous carbon and nitrogen-doped carbon from poly (ethylene oxide-*b*-caprolactone) diblock copolymers. *Chem Eur J* 23:13734–13741
26. Wei J, Zhou D, Sun Z, Deng Y, Xia Y, Zhao D (2013) A controllable synthesis of rich nitrogen-doped ordered mesoporous carbon for CO<sub>2</sub> capture and supercapacitors. *Adv Funct Mater* 23(18):2322–2328
27. Liang C, Hong K, Guiochon GA, Mays JW, Dai S (2004) Synthesis of a large-scale highly ordered porous carbon film by self-assembly of block copolymers. *Angew Chem Int Ed* 43(43):5785–5789
28. Jayaramulu K, Dubal DP, Nagar B, Ranc V, Tomanec O, Petr M, Datta KKR, Zboril R, Gómez-Romero P, Fischer RA (2018) Ultrathin hierarchical porous carbon nanosheets for high-performance supercapacitors and redox electrolyte energy storage. *Adv Mater* 30(15):1705789
29. Yu S, Sun N, Hu L, Wang L, Zhu Q, Guan Y, Xu B (2018) Self-template and self-activation synthesis of nitrogen-doped hierarchical porous carbon for supercapacitors. *J Power Sources* 405:132–141

30. Xu F, Tang Z, Huang S, Chen L, Liang Y, Mai W, Zhong H, Fu R, Wu D (2015) Facile synthesis of ultrahigh-surface-area hollow carbon nanospheres for enhanced adsorption and energy storage. *Nat Commun* 6(1):1–12
31. Pandolfo AG, Hollenkamp AF (2006) Carbon properties and their role in supercapacitors. *J Power Sources* 157(1):11–27
32. Yang D, Ionescu MI (2017) Metal oxide–carbon hybrid materials for application in supercapacitors. In: *Metal oxides in supercapacitors*. Elsevier, pp 193–218
33. Sing KS (1985) Reporting physisorption data for gas/solid systems with special reference to the determination of surface area and porosity (Recommendations 1984). *Pure Appl Chem* 57(4):603–619
34. Yang H, Ye S, Zhou J, Liang T (2019) Biomass-derived porous carbon materials for supercapacitor. *Front Chem* 7(274):1–17
35. Sevilla M, Fuertes AB (2014) Direct synthesis of highly porous interconnected carbon nanosheets and their application as high-performance supercapacitors. *ACS Nano* 8(5):5069–5078
36. Jang M, Ko D, Choi Y, Yan B, Jin X, Kim DK, Piao Y (2021) Self-organized hierarchically porous carbon coated on carbon cloth for high-performance freestanding supercapacitor electrodes. *J Electroanal Chem* 895:115456
37. Ran F, Yang X, Xu X, Li S, Liu Y, Shao L (2021) Green activation of sustainable resources to synthesize nitrogen-doped oxygen-rich porous carbon nanosheets towards high-performance supercapacitor. *Chem Eng J* 412:128673
38. Chmiola J, Yushin G, Gogotsi Y, Portet C, Simon P, Taberna PL (2006) Anomalous increase in carbon capacitance at pore sizes less than 1 nanometer. *Science* 313(5794):1760–1763
39. Raymundo-Pinero E, Kierzek K, Machnikowski J, Béguin F (2006) Relationship between the nanoporous texture of activated carbons and their capacitance properties in different electrolytes. *Carbon* 44(12):2498–2507
40. Deng Y, Ji Y, Wu H, Chen F (2019) Enhanced electrochemical performance and high voltage window for supercapacitor based on multi-heteroatom modified porous carbon materials. *Chem Commun* 55(10):1486–1489
41. Poochai C, Srikaow A, Lohitkarn J, Kongthong T, Tuantranont S, Tuantranont S, Primpray V, Maeboonruan N, Wisitsoraat A, Sriprachuabwong C (2021) Waste coffee grounds derived nanoporous carbon incorporated with carbon nanotubes composites for electrochemical double-layer capacitors in organic electrolyte. *J Energy Storage* 43:103169
42. Chen Z, Wang X, Ding Z, Wei Q, Wang Z, Yang X, Qiu J (2019) Biomass-based hierarchical porous carbon for supercapacitors: effect of aqueous and organic electrolytes on the electrochemical performance. *ChemSusChem* 12(23):5099–5110
43. Miao L, Song Z, Zhu D, Li L, Gan L, Liu M (2021) Ionic liquids for supercapacitive energy storage: a mini-review. *Energy Fuels* 35(10):8443–8455
44. Xia M, Zhang X, Chen Y, Sun F, Wang X, Yang H, Chen H (2020) Hierarchical porous carbon derived from wood tar using crab as the template: performance on supercapacitor. *J Power Sources* 455:227982
45. Wang D, Fang G, Geng G, Ma J (2017) Unique porous carbon constructed by highly interconnected nanowalls for high-performance supercapacitor in organic electrolyte. *Mater Lett* 189:50–53
46. Li C, Zhang X, Wang K, Sun X, Liu G, Li J, Tian H, Li J, Ma Y (2017) Scalable self-propagating high-temperature synthesis of graphene for supercapacitors with superior power density and cyclic stability. *Adv Mater* 29(7):1604690
47. Nguyen QD, Patra J, Hsieh CT, Li J, Dong QF, Chang JK (2018) Supercapacitive properties of micropore- and mesopore-rich activated carbon in ionic liquid electrolytes with various constituent ions. *ChemSusChem* 12(2):449–456
48. Wu Y, Cao JP, Zhuang QQ, Zhao XY, Zhou Z, Wei YL, Zhao M, Bai HC (2021) Biomass-derived three-dimensional hierarchical porous carbon network for symmetric supercapacitors with ultra-high energy density in ionic liquid electrolyte. *ElectrochimActa* 371:137825

49. Na W, Jun J, Park JW, Lee G, Jang J (2017) Highly porous carbon nanofibers co-doped with fluorine and nitrogen for outstanding supercapacitor performance. *J Mater Chem A* 5(33):17379–17387
50. Cai J, Niu H, Wang H, Shao H, Fang J, He J, Xiong H, Ma C, Lin T (2016) High-performance supercapacitor electrode from cellulose-derived, inter-bonded carbon nanofibers. *J Power Sources* 324:302–308
51. Berenguer R, García-Mateos FJ, Ruiz-Rosas R, Cazorla-Amorós D, Morallón E, Rodríguez-Mirasol J, Cordero T (2016) Biomass-derived binderless fibrous carbon electrodes for ultrafast energy storage. *Green Chem* 18(6):1506–1515
52. Ouyang T, Cheng K, Yang F, Zhou L, Zhu K, Ye K, Wang G, Cao D (2017) From biomass with irregular structures to 1D carbon nanobelts: a stripping and cutting strategy to fabricate high performance supercapacitor materials. *J Mater Chem A* 5(28):14551–14561
53. Jin Z, Yan X, Yu Y, Zhao G (2014) Sustainable activated carbon fibers from liquefied wood with controllable porosity for high-performance supercapacitors. *J Mater Chem A* 2(30):11706–11715
54. Fan X, Yu C, Yang J, Ling Z, Hu C, Zhang M, Qiu J (2015) A layered-nanospace-confinement strategy for the synthesis of two-dimensional porous carbon nanosheets for high-rate performance supercapacitors. *Adv Energy Mater* 5(7):1401761
55. Xu Y, Sprick RS, Brownbill NJ, Blanc F, Li Q, Ward JW, Ren S, Cooper AI (2021) Bottom-up wet-chemical synthesis of a two-dimensional porous carbon material with high supercapacitance using a cascade coupling/cyclization route. *J Mater Chem A* 9(6):3303–3308
56. Zhao Q, Wang X, Liu J, Wang H, Zhang Y, Gao J, Lu Q, Zhou H (2015) Design and synthesis of three-dimensional hierarchical ordered porous carbons for supercapacitors. *ElectrochimActa* 154:110–118
57. Li Z, Zhang L, Chen X, Li B, Wang H, Li Q (2019) Three-dimensional graphene-like porous carbon nanosheets derived from molecular precursor for high-performance supercapacitor application. *ElectrochimActa* 296:8–17
58. Gogotsi Y, Penner RM (2018) Energy storage in nanomaterials—capacitive, pseudocapacitive, or battery-like? *ACS Nano* 12(3):2081–2083
59. Wang Q, Yan J, Fan Z (2016) Carbon materials for high volumetric performance supercapacitors: design, progress, challenges and opportunities. *Energy Environ Sci* 9(3):729–762
60. Wang Q, Yan J, Fan Z (2014) Nitrogen-doped sandwich-like porous carbon nanosheets for high volumetric performance supercapacitors. *ElectrochimActa* 146:548–555
61. Yan X, Yu Y, Ryu SK, Lan J, Jia X, Yang X (2014) Simple and scalable synthesis of phosphorus and nitrogen enriched porous carbons with high volumetric capacitance. *ElectrochimActa* 136:466–472
62. Hu J, Wang H, Gao Q, Guo H (2010) Porous carbons prepared by using metal–organic framework as the precursor for supercapacitors. *Carbon* 48(12):3599–3606
63. Raymundo-Piñero E, Leroux F, Béguin F (2006) A high-performance carbon for supercapacitors obtained by carbonization of a seaweed biopolymer. *Adv Mater* 18(14):1877–1882
64. Xu B, Wu F, Chen S, Zhou Z, Cao G, Yang Y (2009) High-capacitance carbon electrode prepared by PVDC carbonization for aqueous EDLCs. *ElectrochimActa* 54(8):2185–2189
65. Tao Y, Xie X, Lv W, Tang DM, Kong D, Huang Z, Nishihara H, Ishii T, Li B, Golberg D, Kang F (2013) Towards ultrahigh volumetric capacitance: graphene derived highly dense but porous carbons for supercapacitors. *Sci Rep* 3(1):1–8
66. Yan L, Li D, Yan T, Chen G, Shi L, An Z, Zhang D (2018) N, P, S-codoped hierarchically porous carbon spheres with well-balanced gravimetric/volumetric capacitance for supercapacitors. *ACS Sustainable Chem Eng* 6(4):5265–5272
67. Jin H, Feng X, Li J, Li M, Xia Y, Yuan Y, Yang C, Dai B, Lin Z, Wang J, Lu J, Wang S (2019) Heteroatom-doped porous carbon materials with unprecedented high volumetric capacitive performance. *Angew Chem Int Ed* 58(8):2397–2401
68. Liang X, Liu R, Wu X (2021) Biomass waste derived functionalized hierarchical porous carbon with high gravimetric and volumetric capacitances for supercapacitors. *Microporous and Mesoporous Mater* 310:110659

69. Xue B, Wang X, Feng Y, Chen Z, Liu X (2020) Self-template synthesis of nitrogen-doped porous carbon derived from rice husks for the fabrication of high volumetric performance supercapacitors. *J Energy Storage* 30:101405
70. Gao H, Zhang D, Zhou H, Wu J, Xu G, Huang Z, Liu M, Yang J, Chen D (2020) Boosting gravimetric and volumetric energy density of supercapacitors by 3D pomegranate-like porous carbon structure design. *Appl Surf Sci* 534:147613
71. Zhu T, Liu S, Wan K, Zhang C, Feng Y, Feng W, Liu T (2020) Fluorine and nitrogen dual-doped porous carbon nanosheet-enabled compact electrode structure for high volumetric energy storage. *ACS Appl Energy Mater* 3(5):4949–4957
72. Helmholtz HV (1853) Uebereinigtesetze der VertheilungelektrischerStröme in körperlichenLeitern, mitAnwendung auf die thierisch-elektrischenVersuche (Schluss.). *Annalen der Physik* 165(7):353–377
73. Lu M (2013) Supercapacitors: materials, systems, and applications. John Wiley & Sons
74. Fedorov MV, Kornyshev AA (2014) Ionic liquids at electrified interfaces. *Chem Rev* 114(5):2978–3036
75. Huang MM, Jiang Y, Sasisanker P, Driver GW, Weingärtner H (2011) Static relative dielectric permittivities of ionic liquids at 25 C. *J Chem Eng Data* 56(4):1494–1499
76. Gouy M (1910) Sur la constitution de la charge électrique à la surface d'un électrolyte. *J Phys Theor Appl* 9(1):457–468
77. Chapman DL (1913) LI. A contribution to the theory of electrocapillarity. *Lond Edinb Dublin Philos Mag J Sci* 25(6):475–481
78. Grahame DC (1947) The electrical double layer and the theory of electrocapillarity. *Chem Rev* 41(3):441–501
79. Bard AJ, Faulkner LR (2001) *Electrochemical methods fundamentals and applications*, 2nd edn. John Wiley & Sons Inc.
80. Stern O (1924) The theory of the electrolytic double-layer. *Z Elektrochem* 30(508):1014–1020
81. Kornyshev AA (2007) Double-layer in ionic liquids: paradigm change? *J Phys Chem B* 111(20):5545–5557
82. Fawcett WR (1979) Molecular models for solvent structure at polarizable interfaces. *Isr J Chem* 18(1–2):3–16
83. Kimizuka O, Tanaike O, Yamashita J, Hiraoka T, Futaba DN, Hata K, Machida K, Suematsu S, Tamamitsu K, Saeki S, Yamada Y (2008) Electrochemical doping of pure single-walled carbon nanotubes used as supercapacitor electrodes. *Carbon* 46(14):1999–2001
84. Geim AK, Novoselov KS (2007) The rise of graphene. *Nat Mater* 6:183–191
85. Jagiello J, Olivier JP (2013) 2D-NLDFT adsorption models for carbon slit-shaped pores with surface energetical heterogeneity and geometrical corrugation. *Carbon* 55:70–80
86. Forse AC, Merlet C, Allan PK, Humphreys EK, Griffin JM, Aslan M, Zeiger M, Presser V, Gogotsi Y, Grey CP (2015) New insights into the structure of nanoporous carbons from NMR, Raman, and pair distribution function analysis. *Chem Mater* 27(19):6848–6857
87. Cychosz KA, Guillet-Nicolas R, García-Martínez J, Thommes M (2017) Recent advances in the textural characterization of hierarchically structured nanoporous materials. *Chem Soc Rev* 46(2):389–414
88. Shi H (1996) Activated carbons and double layer capacitance. *ElectrochimActa* 41(10):1633–1639
89. Gamby J, Taberna PL, Simon P, Fauvarque JF, Chesneau M (2001) Studies and characterisations of various activated carbons used for carbon/carbon supercapacitors. *J Power Sources* 101(1):109–116
90. Endo M, Maeda T, Takeda T, Kim YJ, Koshiba K, Hara H, Dresselhaus MS (2001) Capacitance and pore-size distribution in aqueous and nonaqueous electrolytes using various activated carbon electrodes. *J Electrochem Soc* 148:A910
91. Barbieri O, Hahn M, Herzog A, Kötz R (2005) Capacitance limits of high surface area activated carbons for double layer capacitors. *Carbon* 43(6):1303–1310
92. Ji H, Zhao X, Qiao Z, Jung J, Zhu Y, Lu Y, Zhang LL, MacDonald AH, Ruoff RS (2014) Capacitance of carbon-based electrical double-layer capacitors. *Nature Commun* 5:1–7

93. Lin C, Ritter JA, Popov BN (1999) Correlation of double-layer capacitance with the pore structure of sol-gel derived carbon xerogels. *J Electrochem Soc* 146(10):3639
94. Lozano-Castello D, Cazorla-Amorós D, Linares-Solano A, Shiraishi S, Kurihara H, Oya A (2003) Influence of pore structure and surface chemistry on electric double layer capacitance in non-aqueous electrolyte. *Carbon* 41(9):1765–1775
95. Li H, Qi C, Tao Y, Liu H, Wang DW, Li F, Yang QH, Cheng HM (2019) Quantifying the volumetric performance metrics of supercapacitors. *Adv Energy Mater* 9(21):1900079
96. Liu T, Zhang F, Song Y, Li Y (2017) Revitalizing carbon supercapacitor electrodes with hierarchical porous structures. *J Mater Chem A* 5(34):17705–17733
97. Xie L, Su F, Xie L, Guo X, Wang Z, Kong Q, Sun G, Ahmad A, Li X, Yi Z, Chen C (2020) Effect of pore structure and doping species on charge storage mechanisms in porous carbon-based supercapacitors. *Mater Chem Front* 4(9):2610–2634
98. Shodiev A, Primo E, Arcelus O, Chouchane M, Osenberg M, Hilger A, Manke I, Li J, Franco AA (2021) Insight on electrolyte infiltration of lithium ion battery electrodes by means of a new three-dimensional-resolved lattice Boltzmann model. *Energy Storage Mater* 38:80–92
99. Li G, Lei W, Luo D, Deng YP, Wang D, Chen Z (2018) 3D porous carbon sheets with multidirectional ion pathways for fast and durable lithium–sulfur batteries. *Adv Energy Mater* 8(8):1702381
100. He Y, Zhang Y, Li X, Lv Z, Wang X, Liu Z, Huang X (2018) Capacitive mechanism of oxygen functional groups on carbon surface in supercapacitors. *ElectrochimActa* 282:618–625
101. Wang H, Fan R, Miao J, Deng J, Wang Y (2019) Oxygen groups immobilized on micropores for enhancing the pseudocapacitance. *ACS Sustainable Chem Eng* 7(13):11407–11414
102. Veerasamy VS, Yuan J, Amaratunga GAJ, Milne WI, Gilkes KWR, Weiler M, Brown LM (1993) Nitrogen doping of highly tetrahedral amorphous carbon. *Phys Rev B* 48(24):17954
103. Kapteijn F, Moulijn JA, Matzner S, Boehm HP (1999) The development of nitrogen functionality in model chars during gasification in CO<sub>2</sub> and O<sub>2</sub>. *Carbon* 37(7):1143–1150
104. Ornelas O, Sieben JM, Ruiz-Rosas R, Morallon E, Cazorla-Amorós D, Geng J, Soïn N, Siores E, Johnson BF (2014) On the origin of the high capacitance of nitrogen-containing carbon nanotubes in acidic and alkaline electrolytes. *Chem Commun* 50(77):11343–11346
105. Liu K, Zheng X, Wang K, Wang C, Chen M (2019) Sodium metal-assisted carbonization of pyrrole to prepare N-doped porous carbons for high-rate performance supercapacitors. *Carbon* 153:265–273
106. Zhu D, Jiang J, Sun D, Qian X, Wang Y, Li L, Wang Z, Chai X, Gan L, Liu M (2018) A general strategy to synthesize high-level N-doped porous carbons via Schiff-base chemistry for supercapacitors. *J Mater Chem A* 6(26):12334–12343
107. Liu Y, Wang Z, Teng W, Zhu H, Wang J, Elzatahry AA, Al-Dahyan D, Li W, Deng Y, Zhao D (2018) A template-catalyzed in situ polymerization and co-assembly strategy for rich nitrogen-doped mesoporous carbon. *J Mater Chem A* 6(7):3162–3170
108. Luo L, Zhou Y, Yan W, Wu X, Wang S, Zhao W (2020) Two-step synthesis of B and N co-doped porous carbon composites by microwave-assisted hydrothermal and pyrolysis process for supercapacitor application. *ElectrochimActa* 360:137010
109. Duan B, Gao X, Yao X, Fang Y, Huang L, Zhou J, Zhang L (2016) Unique elastic N-doped carbon nanofibrous microspheres with hierarchical porosity derived from renewable chitin for high rate supercapacitors. *Nano Energy* 27:482–491
110. Wu X, Jiang L, Long C, Fan Z (2015) From flour to honeycomb-like carbon foam: carbon makes room for high energy density supercapacitors. *Nano Energy* 13:527–536
111. Lu Y, Liang J, Deng S, He Q, Deng S, Hu Y, Wang D (2019) Hypercrosslinked polymers enabled micropore-dominant N, S Co-Doped porous carbon for ultrafast electron/ion transport supercapacitors. *Nano Energy* 65:103993
112. Xu Z, Zhuang X, Yang C, Cao J, Yao Z, Tang Y, Jiang J, Wu D, Feng X (2016) Nitrogen-doped porous carbon superstructures derived from hierarchical assembly of polyimide nanosheets. *Adv Mater* 28(10):1981–1987
113. Pachfule P, Shinde D, Majumder M, Xu Q (2016) Fabrication of carbon nanorods and graphene nanoribbons from a metal–organic framework. *Nat Chem* 8(7):718–724

114. Wang JG, Liu H, Zhang X, Shao M, Wei B (2018) Elaborate construction of N/S-co-doped carbon nanobowls for ultrahigh-power supercapacitors. *J Mater Chem A* 6(36):17653–17661
115. Tian J, Zhang H, Liu Z, Qin G, Li Z (2018) One-step synthesis of 3D sulfur-doped porous carbon with multilevel pore structure for high-rate supercapacitors. *Int J Hydrogen Energy* 43(3):1596–1605
116. Niu Q, Gao K, Tang Q, Wang L, Han L, Fang H, Zhang Y, Wang S, Wang L (2017) Large-size graphene-like porous carbon nanosheets with controllable N-doped surface derived from sugarcane bagasse pith/chitosan for high performance supercapacitors. *Carbon* 123:290–298
117. Wang T, Sun Y, Zhang L, Li K, Yi Y, Song S, Li M, Qiao ZA, Dai S (2019) Space-confined polymerization: controlled fabrication of nitrogen-doped polymer and carbon microspheres with refined hierarchical architectures. *Adv Mater* 31(16):1807876
118. Yu J, Yu C, Guo W, Wang Z, Li S, Chang J, Tan X, Ding Y, Zhang M, Yang L, Xie Y (2019) Decoupling and correlating the ion transport by engineering 2D carbon nanosheets for enhanced charge storage. *Nano Energy* 64:103921
119. Zhang W, Cheng R, Wang Z, Ma Y, Ran S, Lv Y, Ma L (2020) A composite-hydroxide-activation strategy for the preparation of N/S dual-doped porous carbon materials as advanced supercapacitor electrodes. *J Mater Sci: Mater Electron* 31(24):22498–22511
120. Deng W, Zhang Y, Yang L, Tan Y, Ma M, Xie Q (2015) Sulfur-doped porous carbon nanosheets as an advanced electrode material for supercapacitors. *RSC Adv* 5(17):13046–13051
121. Yang L, Wu D, Wang T, Jia D (2020) B/N-codoped carbon nanosheets derived from the self-assembly of chitosan–amino acid gels for greatly improved supercapacitor performances. *ACS Appl Mater Interfaces* 12(16):18692–18704
122. Yao L, Wu Q, Zhang P, Zhang J, Wang D, Li Y, Ren X, Mi H, Deng L, Zheng Z (2018) Scalable 2D hierarchical porous carbon nanosheets for flexible supercapacitors with ultrahigh energy density. *Adv Mater* 30:1706054